# Inverted p-down pin photodiode exceeding 70-GHz bandwidth featuring low operating bias voltage of 2 V

Masahiro Nada(1), Fumito Nakajima(2), Shoko Tatsumi(1), Yuki Yamada(2), Yasuhiko Nakanishi(1), Toshihide Yoshimatsu(1), Kimikazu Sano(1) and Hideaki Matsuzaki(2)

(1) NTT Device Innovation Center, NTT Corporation, masahiro.nada.fb@hco.ntt.co.jp
(2) NTT Device Technology Laboratories, NTT Corporation

**Abstract** *We present a vertical-illumination pin photodiode (PD) with an inverted p-down structure, which is advantageous in fabrication, optical coupling, and dark-current suppression. The PD is designed to maximize bandwidth at low bias, resulting in 70.1-GHz bandwidth at 2 V with 0.61-A/W responsivity.*

## Introduction

The continuous growth of data traffic has pushed baud rates higher. While the industrial side is starting to develop practical systems using 50-Gbaud transmission as represented by 100-Gbit/s PAM4, the quest for 100-Gbaud systems has begun on the research side. Photodiodes (PDs) with higher bandwidths are also anticipated to meet these demands. Typical attempts to realize such ultrahigh-speed PDs are based on waveguide designs that allows both a long optical path in the absorber and short carrier transit time to simultaneously obtain larger bandwidth and responsivity [1-3].

In this paper, we present a vertical-illumination PD, as opposed to the waveguide-type high-speed PD, which is advantageous in terms of optical coupling, fabrication complexity, and polarization dependence. The vertical-illumination PD features an inverted p-down configuration that provides a low dark current. It also features an optimized electric-field profile to maximize the bandwidth at a low operating bias voltage. The fabricated PD exhibited the bandwidth of up to 70.1 GHz with a responsivity of 0.61 A/W for a 1.3-µm input signal at 2 V. Dark current as low as 0.84 nA is maintained even at a bias voltage of 10 V.

## Design of inverted p-down PD

Generally, the intrinsic bandwidth of PDs is governed by both the thickness of the depleted layers where the electrons and holes travel and the drift velocities of those carriers. It is well known that electrons in an InGaAs absorber show maximum drift velocity under the electric field of 10-15 kV/cm [4-5], and then the electron drift velocity gradually decreases with the additional increase in the electric field. On the other hand, the hole drift velocity in InGaAs does not have such an overshoot. That is, it gradually increases as the electric field increases and saturates at the electric field of approximately 50 kV/cm [6]. From the viewpoint of the high-speed drift of holes, the electric field in InGaAs should be over 50 kV/cm; however, an excessive electric field degrades the electron velocity. Thus, to maximize the bandwidth of pin PDs, we have to carefully design the layer structure to ensure saturated hole velocity and large electron velocity at a desired bias voltage.

We set the target operating bias voltage to 2 V, considering a practical application of the inverted p-down PD to optical receivers integrated with electrical amplifiers. Figure 1 shows the schematic cross section of the inverted p-down PD. The basic structure is similar to that our previously reported inverted p-down avalanche photodiodes [7-9]. The layer structure, which is grown on an InP substrate, includes a p-type contact layer, a 450-nm-thick hybrid absorber consisting of p-type and undoped InGaAs, an InP collector layer, and an n-type contact layer. After the epitaxial growth, a triple-mesa shape is formed by conventional wet etching. A mirror metal is deposited on the n-type contact layer. After the PD fabrication, the InP substrate is thinned down, and an AR film is coated on its back side. The fabricated PD thus has a backside-illumination and two-path structure.

The top mesa consisting of the n-type contact layer defines active area of the inverted p-down PD. We prepared PDs with various active diameters to characterize the dark current and OE response.

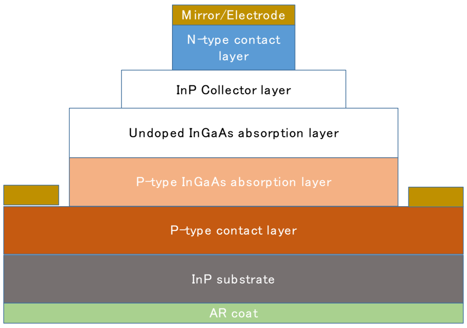


**Fig. 1: Schematic cross section of the inverted p-down PD**

## Device performance

Figure 2 shows I-V characteristics of a fabricated PD with an active area diameter of 10 μm. In the photocurrent measurement, optical input power was -4 dBm at the wavelength of 1300 nm.

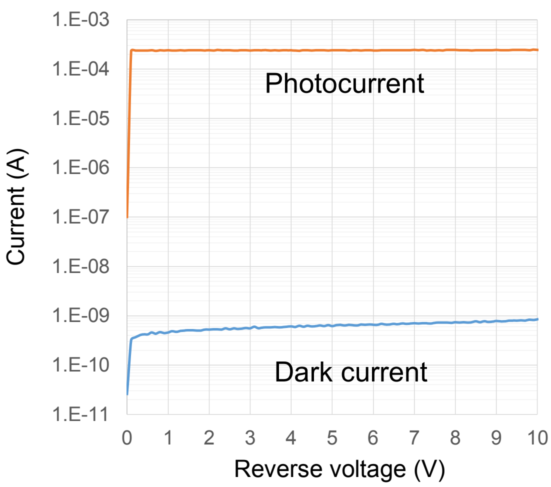


**Fig. 2: I-V characteristics of the fabricated inverted p-down PD with 10-μm active area diameter**

The responsivity was 0.61 A/W, while the dark current was 0.52 nA at 2 V. Notably, dark current as low as 0.84 nA was maintained even at 10 V. This indicates weak bias voltage dependence of the dark current in a large bias voltage range up to 10 V, which well reflects the advantage of the inverted p-down structure. As described in [8, 10], the electric field on the sidewall of the device is maintained at approximately zero regardless of the applied bias voltage. In other words, the bias voltage applied to the inverted p-down PD only contributes to enhancing the electric field in the active area, which results in drastic suppression of surface leakage current.

Figure 3 shows the active-area dependence of the dark current of the fabricated inverted p-down PDs. If the dark current is due to surface leakage, it should be proportional to the square root of the active area, while it should be proportional to the active area if its origin is tunneling current or generation-recombination current. Clearly, the measured dark current depends on neither the active area nor the square root of it even when the bias voltage is 10 V. Therefore, it can be said that the inverted p-down PD has practically negligible dark-current components induced by the electric field, which is advantageous in terms of PD reliability and stability.

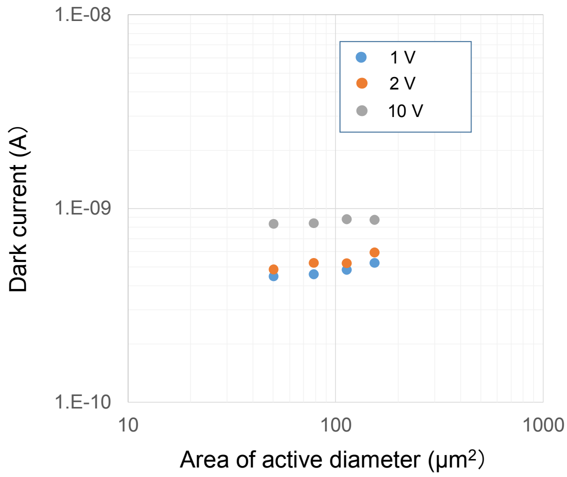


**Fig. 3: Active area dependences of the dark current of the inverted p-down PD for 1, 2, and 10 V.**

Figure 4 shows the OE response of fabricated inverted p-down PDs with active area diameters of 10 and 14 μm at 2 V. The optical input was -4 dBm with a 1300-nm wavelength. Owing to the limitation of the optical component analyzer we used, the measurement was carried out in the frequency range from 0.05 to 49.8 GHz. The 10-μm device exhibited a 3-dB down bandwidth exceeding 49.8 GHz. We roughly estimated the 3-dB down bandwidth with a fitting formula of $1/(1+j\omega\tau)$ as shown in Fig. 4. The estimated 3-dB down bandwidth of the 10-μm device is 70.1 GHz, while that of the 14-μm device is 39.0 GHz.

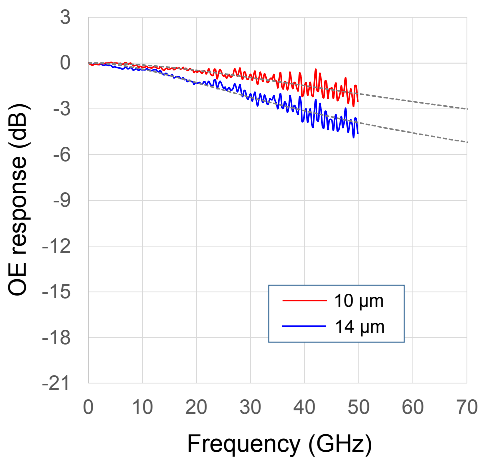


**Fig. 4: Frequency characteristics of the inverted p-down PDs with 10- and 14-um diameters**

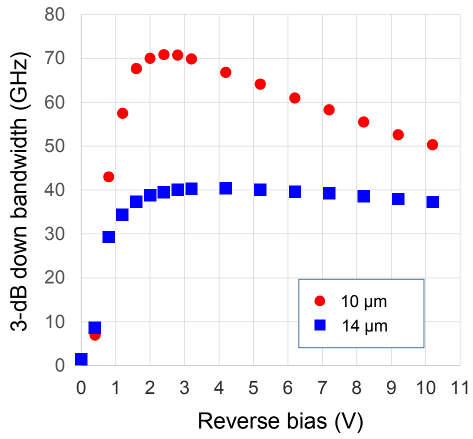


**Fig. 5: Bias dependence of the 3-dB down bandwidth for fabricated devices with the active area diameters of 10 and 14 µm**

Finally, to clarify the effectiveness of our designed layer structure for maximizing the operating bandwidth at 2 V, we measured the bias dependence of the 3-dB down bandwidth of the devices with diameters of 10- and 14-µm. As shown in Figure 5, the bandwidth of both devices is almost zero at bias voltage of 0, and then it rapidly increases as the applied bias voltage increases. The bandwidth of the 10-µm device is 70.1 GHz at 2.0 V, and it reaches 70.9 GHz at 2.4 V. At this bias condition, the electric field in the depleted layers is estimated to be approximately 60 kV/cm. This is reasonable in terms of the hole velocity characteristics against the electric filed as described in [6]. Then the bandwidth gradually degrades as the bias voltage increases, owing to saturation of the electron velocity.

For the 14-µm device, the bias voltage dependence of the bandwidth is significantly weakened; once the bandwidth increases, it is almost maintained at least up to 10.2 V. The peak bandwidth of the 14-µm is 40.4 GHz at 4.2 V, and then it decreases to 37.2 GHz at 10.2 V. This is because the CR time constant is dominant compared to the change in electron velocity against the increase in electric field. At 3.3 V, the typical operating bias voltage of PDs when the bias is provided through trans-impedance amplifier, the bandwidths are respectively 69.9 and 40.3 GHz for the 10- and 14-µm devices.

## Conclusions

We designed and fabricated an inverted p-down PD, which features low dark current and easy optical coupling and fabrication. The fabricated device exhibited dark current as low as 0.52 nA at 2 V, which is maintained at less than 1 nA at the bias voltage of 10 V. Furthermore, the dark current shows weak dependence on the active area of the devices, indicating that the inverted p-down PDs show marginal dark current associated with the electric field. This is a unique advantage in terms of reliability and stability. Owing to the optimized layer structure, the operation bandwidth of a 10-µm device reaches over 70 GHz at bias voltage as low as 2 V, and the responsivity of 0.61 A/W for the wavelength of 1300 nm in spite of the vertical-illumination configuration. The bias voltage dependence of the bandwidth of the 10-µm device is well explained by the hole saturation velocity and electron-velocity degradation, showing the importance of the management of the electric field in the depleted layers at an operating bias condition.

## References


[1] K. Kato *et al.*, "110-GHz, 50%-efficiency mushroom-mesa waveguide p-i-n photodiode for a 1.55-µm wavelength", *IEEE Photon. Technol. Lett.*, vol. 6, no. 6, pp. 719–721, 1994.

[2] P. Runge *et al.*, "Broadband 145GHz Photodetector Module Targeting 200GBaud Applications", in *Proc. The Optical Fiber Communication Conference (OFC'2020)*, San Diego, CA, USA, Mar. 2020, M2A.1.

[3] A. Beling and J. Campbell, "High-speed Photodiodes", *IEEE J. Sel. Topics Quantum Electron.,* vol. 20, no. 6, p. 3804507, 2014.

[4] T. H. Windhorn. "Temperature dependent electron velocity-field characteristics for InGaAs at high electric fields", *J. Electron. Materials,* vol. 11, no. 6, pp. 1065–

1082, 1982.

[5] T. Ishibashi et al., ”High speed heterostructure devices”, *in Semiconductors and Semimaterials*. San Diego, CA, Academic, 1994, vol. 41, ch. 5, p. 333.

[6] P. Hill, et al., “Measurement of hole velocity in n-type InGaAs”, *Appl. Phys. Lett.*, vol. 50, no. 1260, 1987.

[7] F. Nakajima et al., “High-Speed Avalanche Photodiode and High-Sensitivity Receiver Optical Subassembly for 100-Gb/s Ethernet”, *J. Lightwave Technol.,* vol. 34, no. 2, pp. 243-248, 2015.

[8] M. Nada et al., “Triple-mesa avalanche photodiode with p-down structure for reliability and stability”, *J. Lightwave Technol*., vol. 32, no. 8, pp. 1543-1548, 2014.

[9] M. Nada et al., “Responsivity-Bandwidth Limit of Avalanche Photodiodes: Toward Future Ethernet Systems”, *J. Sel. Topics Quantum Electron.,* vol. 24, no. 2, p. 3800811, 2016.

[10] Y. Yuan et al., “Triple-mesa avalanche photodiodes with very low surface dark current”, *Optics Express,* vol. 27, no. 16, p. 22923, 2019/